THYROID
Volume 24, Number 7, 2014
© Mary Ann Liebert, Inc.
DOI: 10.1089/thy.2013.0676

Apoptosis of NOD.H2^{h4} Thyrocytes by Low Concentrations of Iodide is Associated with Impaired Control of Oxidative Stress

Panayota Kolypetri and George Carayanniotis

Background: Enhanced iodide intake in NOD.H2^{h4} mice accelerates the incidence and severity of spontaneous autoimmune thyroiditis (SAT) via an unknown mechanism. A plausible hypothesis is that iodide-induced apoptosis of thyrocytes can create imbalances in antigenic load and/or disruption of immunoregulatory mechanisms that facilitate activation of autoreactive T cells in cervical lymph nodes draining the thyroid.
Methods: We examined whether NOD.H2^{h4} thyrocytes, exposed to low NaI concentrations *in vitro*, are more susceptible to apoptosis compared to thyrocytes from CBA/J mice, which are resistant to iodide-accelerated SAT (ISAT). We also looked, at the transcriptional level, for differential activation of genes involved in apoptosis or oxidative stress pathways that may account for potential differences in iodide-mediated apoptosis between NOD.H2^{h4} and CBA/J thyrocytes.
Results: We report that NOD.H2^{h4} thyrocytes, cultured for 24 h at very low (4–8 μM) concentrations of NaI, exhibit high levels (40–55%) of apoptosis, as assessed microscopically following staining with fluorescent caspase inhibitors. Similar treatment of thyrocytes from CBA/J mice, which are resistant to ISAT, yielded significantly lower (10–20%) apoptotic rates. Expression analysis by real-time polymerase chain reaction using arrays of apoptosis- and oxidative stress-related genes showed that NaI intake upregulates the expression of 22 genes involved in ROS metabolism and/or antioxidant function in CBA/J thyrocytes, whereas only two of these genes were upregulated in NOD.H2^{h4} thyrocytes. Among the set of overexpressed genes were those encoding thyroid peroxidase (*Tpo*; 5.77-fold), glutathione peroxidases (*Gpx2*, *Gpx4*, *Gpx7*; 2.03–3.14-fold), peroxiredoxins (*Prdx1*, *Prdx2*, *Prdx5*; 2.27–2.97-fold), superoxide dismutase 1 (*Sod1*; 3.57-fold), thioredoxin 1 (*Txn1*; 2.13-fold), and the uncoupling proteins 2 and 3 (*Ucp2*, *Ucp3*; 2.01–2.15-fold).
Conclusions: The results demonstrate that an impaired control of oxidative stress mechanisms is associated with the observed high susceptibility of NOD.H2^{h4} thyrocytes to NaI-mediated apoptosis, and suggest a contributing factor for the development of ISAT in this strain.

Introduction

The NOD.H2^{h4} mouse strain has been well established as an animal model for the study of spontaneous autoimmune thyroiditis (SAT). This strain was originally made in 1993 to investigate potential effects of H-2 region genes on diabetes, but it was serendipitously found to develop only insulitis and not diabetes (1) and showed a much higher incidence of SAT of 50% compared to 5% in NOD mice (2,3). The high incidence of SAT in this strain, carrying the K^k, A^k, E^0, D^b haplotype, has been attributed in part to the combined presence of the A^k molecule, which is permissive for thyroiditis development (4), and NOD non-MHC genes that are known to predispose to autoimmunity (5). SAT appears after 15 weeks of age, and its incidence and severity increase progressively with time. However, when 6–8 week old NOD.H2^{h4} mice are given drinking water containing 0.05% NaI, SAT becomes detectable as early as 2 weeks after the initiation of the dietary regimen and plateaus within 4–8 weeks. The discovery of iodide-accelerated SAT (ISAT) in NOD.H2^{h4} mice complements similar earlier observations of thyroiditis induction by iodide in NOD mice (6,7), BB/W rats (8), and obese strain chickens (9). These animal models strongly suggest an interplay between dietary (environmental) and genetic factors in the activation of an autoimmune response and are likely to involve processes similar to those that precipitate the development of autoimmune thyroiditis and hypothyroidism in humans following excessive iodine intake (10–12).

Intrathyroidal infiltration by mononuclear cells and production of thyroglobulin (Tg)-specific IgG antibodies have

Divisions of Endocrinology and Biomedical Sciences, Faculty of Medicine, Memorial University of Newfoundland, St. John's, Canada.

been well established as the cardinal symptoms of ISAT in NOD.H2^{h4} mice (6,13,14), but the early events whereby iodide triggers the autoimmune cascade remain unknown. Thyrocytes actively take up iodide through the NaI symporter (15), and it is well known that their exposure to high concentrations of iodide can induce their apoptosis or necrosis *in vivo* (9,16–18) or *in vitro* (19–22). A plausible hypothesis is that iodide-induced apoptosis of thyrocytes can create imbalances in antigenic load and/or disruption of immunoregulatory mechanisms that facilitate activation of autoreactive T cells in cervical lymph nodes draining the thyroid. In this report, we examine whether NOD.H2^{h4} thyrocytes, exposed to low NaI concentrations *in vitro*, are more susceptible to apoptosis compared to thyrocytes from CBA/J mice, which are resistant to ISAT (23). We also looked, at the transcriptional level, for differential activation of genes involved in apoptosis or oxidative stress pathways that may account for potential differences in iodide-mediated apoptosis between NOD.H2^{h4} and CBA/J thyrocytes.

Materials and Methods

Animals

NOD.H2^{h4} mice, originally derived by Dr. L. Wicker (Merck Laboratories, Rahway, NJ), were kindly provided by Dr. H. Braley-Mullen (University of Missouri, Columbia, MO). The mice were bred and maintained in the animal facility of the Faculty of Medicine, Memorial University of Newfoundland. Both male and female NOD.H2^{h4} mice were used in the experiments. Female 6–8 week old CBA/J mice were purchased from Jackson Laboratories (Bar Harbor, ME). All experimental procedures were reviewed and approved by the Animal Care Committee at the Memorial University of Newfoundland.

Primary mouse thyrocyte cultures

Thyroid cells were isolated and cultured according to a modified method (24). Thyroid lobes from mice were aseptically removed from the trachea, cut into small fragments, and teased apart, and material from three glands was placed in 1 mL Dulbecco's modified Eagle's medium (DMEM) digestion medium (Gibco, Life Technologies, Grand Island, NY) containing 1 U/mL of collagenase type I (Sigma-Aldrich, St. Louis, MO) and 1.2 U/mL of dispase I (Sigma-Aldrich). Enzymatic digestion was performed at 37°C for 45 min followed by vigorous pipetting. The cells were then washed twice and were resuspended in F-12 Nutrient Mixture (HAM) culture medium (Invitrogen, Carlsbad, CA) supplemented with BD^{TM} Nu-Serum IV Replacements (BD Biosciences, Bedford, MA; diluted 2.5×), glycyl-L-histidyl-L-lysine acetate salt (2 ng/mL final), somatostatin (10 ng/mL), thyrotropin (TSH; 10 mU/mL), and NaI (1 μM all from Sigma). To ascertain purity, thyrocytes were cultured as described above in eight-well chamber slides (Nalge Nunc International, Rochester, NY) using material from three NOD.H2^{h4} thyroid glands per well. On day 10, cells were fixed with acetone for 10 min at −20°C, washed, and subsequently were placed in phosphate-buffered saline containing 10% fetal calf serum for 20 min at room temperature (blocking step). Then, cells were incubated with Tg-specific antisera from iodide-fed NOD.H2^{h4} mice or antisera from control CBA/J mice (1:20 dilution) for 1 h. The cells were then washed three times and incubated with a secondary FITC-labeled goat anti-mouse IgG (Jackson Immunoresearch Laboratories, West Grove, PA) for 30 min. Cells were again washed three times, and one drop of VECTASHIELD Hard-Set Mounting Medium with DAPI (Vector Laboratories, Burlingame, CA) was added to each well. Fluorescent cells were viewed using a Carl Zeiss AxioImager Z.1 microscope.

Microscopic detection of apoptosis

Cells from 10 thyroid glands were added into 18 wells of black 96-well plates (Costar #3603, Corning Incorporated, NY) and were cultured for 10 days at 37°C, 5% CO_2. Medium was changed one day later and then every third day. On day 9, the plates were centrifuged, and cells were washed twice to remove nonadherent, floating cells. Then, various concentrations of NaI (Sigma) or 6 μM camptothecin (Sigma) were added to the cells for 24 h. Apoptosis was assessed by the FAM-FLICA^{TM} *in vitro* Poly Caspases kit (Immunochemistry Technologies, Bloomington, MN), which utilizes a 3-aminoacid sequence (VAD) sandwiched between carboxyfluorescein (FAM) and fluoromethylketone (FMK). The FAM-VAD-FMK reagent penetrates the cell membrane and binds irreversibly to activated caspases 1, 3, 4, 5, 6, 7, 8, and 9. During the last 5 min, propidium iodide and Hoechst 33342 were also added to the wells. After extensive washing (10×), live cells were observed under an inverted Carl Zeiss AxioObserver A.1 microscope. Images were captured using a Zeiss AxioCam MRM3 camera with Zeiss Axiovision 4.8 Software. At least 300 cells per group were counted and analyzed by the ImageJ 1.41 Software (NIH, Bethesda, MD). Statistical analysis of data was performed using the GraphPad Prism v4.01 software.

Expression analysis of apoptosis and oxidative-stress related genes by real-time polymerase chain reaction

The expression of 168 genes involved in apoptotic and oxidative stress-related pathways was measured by the mouse apoptosis and oxidative stress polymerase chain reaction (PCR) arrays (Qiagen Sciences, MD). Thyroid glands from 80 NOD.H2^{h4} and 80 CBA/J mice were isolated and cultured as described above. On day 9, thyrocytes were incubated with or without iodide (4×10^{-6} M final concentration) for 24 h. Then, the supernatant of cultured thyrocytes was removed, and the cells were lysed by the addition of Trizol (Invitrogen). The aqueous phase was mixed with an equal volume of 70% ethanol, and subsequently the sample was transferred to an RNeasy spin column (Qiagen, Cat. #74104). The RNA was purified following on-column DNase treatment (RNase-free DNase set, Qiagen, Cat. #79254) according to the manufacturer's instructions. RNA purity was quantified by spectrophotometry at 260/230 nm and 260/280 nm ratios. The cDNA was transcribed from 1 μg total RNA per group using the RT^2 First Strand Kit (Qiagen, Cat. #330401) in a total volume of 222 μL. Next, 102 μL of cDNA (equivalent to 0.5 μg RNA) were mixed with 1350 μL RT^2 SYBR Green Mastermix and RNase-free water in a total volume of 2700 μL. Twenty-five μL of this PCR components mix were added to each well of the RT^2 Profiler PCR array, and quantitative PCR was performed using a StepOnePlus

Applied Biosystems cycler. The cycling conditions were 95°C for 10 min for activation of HotStart DNA Taq polymerase, followed by 40 cycles of denaturation at 95°C for 15 sec and annealing at 60°C for 60 sec. A dissociation (melting) curve analysis was performed to verify PCR specificity. Each 96-well plate contained primers for 84 pathway-related genes and five housekeeping genes, whereas seven wells contained reverse-transcription controls, positive PCR controls, and genomic DNA contamination control. For each gene of interest, the difference (ΔC_T) between its C_T value and the average C_T value of the five housekeeping control genes was calculated. For each pair-wise set of samples to be compared, the ΔC_T values were calculated as: $\Delta\Delta C_T = \Delta C_T$ (exp) $- \Delta C_T$ (control) and the fold-change of target gene expression was calculated as $2^{(-\Delta\Delta CT)}$. Fold change values of <1 are expressed as negative inverse of fold change.

Results

Establishment of primary thyroid epithelial cell culture and assessment of apoptosis

Single cell suspensions from NOD.H2^{h4} thyroid glands were prepared and cultured for 10 days in complete Ham F-12 medium promoting epithelial cell growth, as described in the Materials and Methods. Using a two-step immunofluorescence assay with FITC-labeled goat anti-mouse IgG, it was shown that >98% of the grown cells were thyrocytes, since their cytoplasm was positively stained by Tg-specific IgG antibodies (Fig. 1A) but remained unstained by normal serum IgG (Fig. 1B). In preliminary experiments, apoptosis of thyrocytes, cultured in the presence of various NaI concentrations, was assessed with the FAM-FLICA^{TM} *in vitro* Poly Caspase kit, which uses a reagent that penetrates the cell membrane and binds irreversibly to activated caspases. With this method, we could readily enumerate healthy (Fig. 1C) versus early or late apoptotic thyrocytes (Fig. 1D and E). Necrotic thyrocytes were identified by staining with propidium iodide (Fig. 1F)

Low concentrations of iodide induce differential apoptosis in NOD.H2^{h4} versus CBA/J thyrocytes

The effect of iodide on NOD.H2^{h4} thyrocyte viability *in vitro* was initially tested within a large range of final NaI concentrations (10^{-5}–10^{-3} M). NaI was added to 9-day cell cultures for 24 h, and subsequently apoptosis was microscopically assessed with the FAM-FLICA assay by counting 300 cells from cultures at each NaI concentration in five independent experiments. It was found that the background apoptosis of thyrocytes grown in the absence of NaI was relatively high (27.12 ± 3.1; percentage mean ± SEM) and that exposure to 10^{-5} M NaI significantly increased the percentage of total apoptotic cells to 58.34 ± 6.3 ($p = 0.021$). This level of apoptosis remained relatively constant over the 10^{-5}–10^{-3} M NaI range and was comparable to that observed following a 12 h treatment of thyrocytes with 6 μM camptothecin (59 ± 3.6). The number of necrotic cells in all

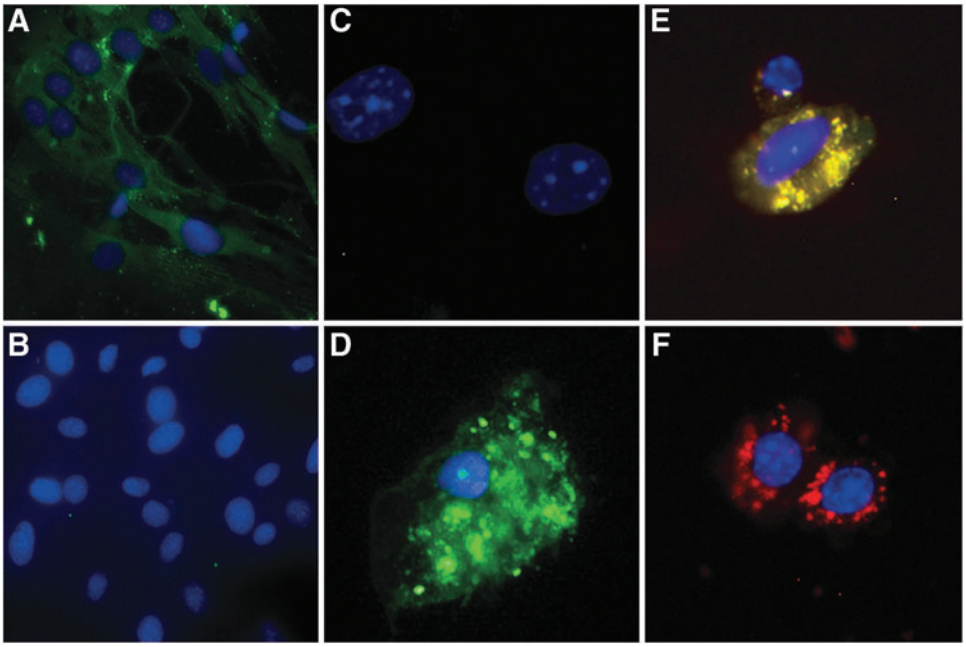

FIG. 1. Establishment of primary mouse thyrocyte cultures and assessment of NaI-induced apoptosis. NOD.H2^{h4} thyrocytes were expanded in culture for 10 days, and their purity was assessed by a two-step immunofluorescence assay using FITC-labeled goat anti-mouse IgG, as described in the Materials and Methods. **(A)** Thyrocytes incubated with NOD.H2^{h4} serum containing high titers of Tg-specific IgG. **(B)** Thyrocytes incubated with control serum from healthy CBA/J mice. Appearance of NOD.H2^{h4} thyrocytes following exposure to apoptotic/necrotic stimuli. **(C)** Healthy thyrocytes (blue staining of nucleus with Hoechst 33342). **(D)** Early apoptotic thyrocyte cultured in 10^{-5} M NaI (green fluorescent staining of cytoplasm with FAM-FLICA poly caspase reagent). **(E)** Late apoptotic thyrocyte cultured in 10^{-5} M NaI (cytoplasmic stain with FAM-FLICA and propidium iodide). **(F)** Necrotic thyrocyte following exposure to 90% ethanol for 30 sec (cytoplasmic stain with propidium iodide).

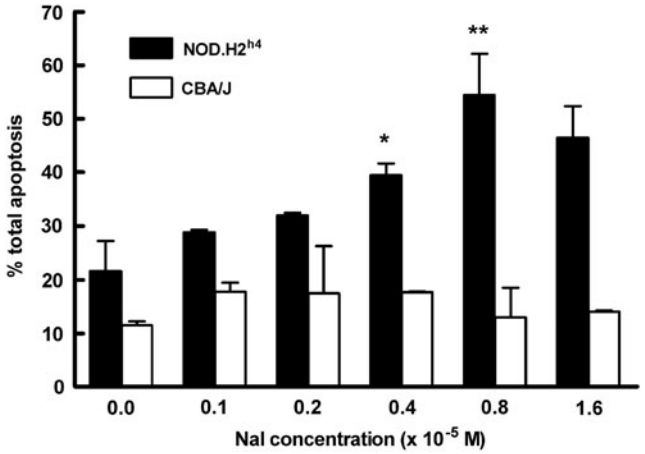

FIG. 2. NOD.H2^{h4} thyrocytes are highly sensitive to iodide-induced apoptosis. Day 9 NOD.H2^{h4} and CBA/J thyrocyte cultures were exposed to the indicated final NaI concentrations for 24 h. Total (early and late) apoptotic cells were microscopically viewed and counted as described in Figure 1, using the FAM-FLICA assay. Three hundred cells were examined per group, and data represent percent apoptosis mean ± standard error of the mean of two independent experiments. The percentage of necrotic cells in all cultures never exceeded 3.4%. Statistical significance was determined by a two-tailed unpaired *t*-test. *$p = 0.051$; **$p = 0.025$.

cultures was negligible. On the basis of these initial data, we selected the 1×10^{-6}–1.6×10^{-5} M NaI range to compare NOD.H2^{h4} versus CBA/J thyrocytes in terms of their susceptibility to iodide-induced apoptosis, since CBA/J mice do not develop ISAT following high NaI intake. As shown in Figure 2, in the absence of NaI, NOD.H2^{h4} thyrocytes showed a background apoptotic rate of 21.59 ± 4.00, which was not significantly higher than that observed in the corresponding CBA/J cell culture (11.5 ± 0.5, $p = 0.128$). However, increasing NaI concentrations induced higher apoptotic rates in NOD.H2^{h4} thyrocytes, peaking at 54.45 ± 5.45 at 8×10^{-6} M NaI. In contrast, over the same molar range of NaI, CBA/J thyrocytes exhibited total apoptotic cell levels that were not significantly higher than those of the control (no NaI) cultures. The percentage of necrotic cells in all cultures was negligible (not shown) and never exceeded 3.4%. Possible osmotic effects were excluded because after exposure to equimolar NaCl concentrations, apoptotic cell rates did not rise above background values (not shown). These data demonstrated that, at low NaI concentrations *in vitro*, NOD.H2^{h4} thyrocytes are more sensitive to iodide-mediated apoptosis than CBA/J thyrocytes, which appeared to be unaffected by the NaI treatment.

Analysis using apoptosis PCR arrays

To investigate further the iodide-mediated apoptosis pathway, we looked at the expression of 84 apoptosis-related genes (Supplementary Table S1; Supplementary Data are available online at www.liebertpub.com/thy) by real time PCR using a mouse Apoptosis PCR array. We first examined whether the number or the relative constitutive expression of pro-apoptotic genes was higher in NOD.H2^{h4} versus CBA/J thyrocytes. Within a set of 35 apoptosis-promoting genes, significant expression differences were observed at eight genes, with two genes (*Tnf* and *TnfSF10*) showing higher expression, and six genes (*Traf 2*, *Trp73*, *Card 10*, *Casp 9*, *Dffb*, and *Casp6*) showing lower expression in NOD.H2^{h4} versus CBA/J/ thyrocytes (Table 1). Conversely, within a set of 26 apoptosis-inhibiting genes, significant expression differences were observed at four genes, with one gene (*Naip2*) showing higher expression (3.29-fold) and three genes (*Nme5*, *Cidea*, and *BCl2l10*) showing lower expression in NOD.H2^{h4} versus CBA/J/ thyrocytes (Table 1). These data did not support the view that NOD.H2^{h4} thyrocytes intrinsically express a clear apoptosis-promoting profile at the gene transcription level, as compared to CBA/J thyrocytes.

Next, we examined the effects of NaI on gene transcription rates in thyrocytes from each strain. After 9 days of culture,

TABLE 1. DIFFERENTIAL EXPRESSION OF APOPTOSIS-RELATED GENES IN NOD.H2^{h4} AND CBA/J THYROCYTES

RefSeq	*Symbol*	*Description*	*Fold change (NOD.H2^{h4}/CBA/J)*[a]
Apoptosis promoting genes			
NM_013693	Tnf	Tumor necrosis factor	3.04
NM_009425	Tnfsf10	Tumor necrosis factor (ligand) superfamily, member 10	2.95
NM_009422	Traf2	Tnf receptor-associated factor 2	−2.01
NM_130859	Card10	Caspase recruitment domain family, member 10	−2.89
NM_015733	Casp9	Caspase 9	−3.03
NM_007859	Dffb	DNA fragmentation factor, beta subunit	−4.01
NM_009811	Casp6	Caspase 6	−23.85
Apoptosis inhibiting genes			
NM_010872	Naip2	NLR family, apoptosis inhibitory protein 2	3.29
NM_080637	Nme5	Nonmetastatic cells 5, protein expressed in (nucleoside-diphosphate kinase)	−2.00
NM_007702	Cidea	Cell death-inducing DNA fragmentation factor, alpha subunit-like effector A	−2.57
NM_013479	Bcl2l10	Bcl-2-like 10	−2.66

[a]A fold change ≥ 2.00 (upregulation) and ≤ −2.00 (downregulation) was considered significant.

cells were treated with 4×10^{-6} M NaI, and RNA from these—and from untreated thyrocyte controls—was extracted 24 h later. Surprisingly, in NOD.H2^{h4} thyrocytes, only the pro-apoptotic gene *Bok* (BCL-2 related ovarian killer protein) showed significant alteration in its expression, as it was completely suppressed (> −500-fold; Supplementary Table S1). Interestingly, the expression of several genes that belong in the Bcl-2 family, and various caspases and their activators, was not significantly affected by the iodide treatment. In NaI-treated CBA/J thyrocytes, there was mild downregulation of five pro-apoptotic genes (*Abl1*, *Dffb*, *RipK1*, *Casp9*, and *Card 10*) and three anti-apoptotic genes (*Bcl2l0*, *Atf5*, and *Il10*) versus the untreated controls (Supplementary Table S1). Only one pro-apoptotic gene (*Tnfsf10*) was upregulated (2.36-fold). Taken together, these data suggest that the apoptosis-enhancing effect of NaI, differentially observed in NOD.H2^{h4} versus CBA/J thyrocytes in Figure 2, could not be clearly attributed to factors operating at the transcriptional level of the genes tested.

Analysis using oxidative stress PCR arrays

Enhanced iodide-induced apoptosis in NOD.H2^{h4} thyrocytes could be triggered by high levels of reactive oxygen species (ROS) that has been reported to be detected in thyrocytes of this strain in the absence of NaI (25). To examine whether NaI-treated or control NOD.H2^{h4} thyrocytes have a defect in the expression of genes participating in ROS metabolism or antioxidant defense mechanisms leading to overproduction of ROS, we performed analysis using an oxidative stress PCR array. The constitutive expression levels of 84 oxidative stress-related genes (Supplementary Table S2) was initially compared between control thyrocytes from the two strains. Significant expression differences were observed for only four genes involved in ROS metabolism, with three genes (*Ncf1*, *Ncf2*, and *Ccl5*) showing higher expression, and one gene (*Duox1*) showing lower expression in the NOD.H2^{h4} group (Table 2). On the other hand, NOD.H2^{h4} thyrocytes significantly overexpressed three genes (*Gpx2*, *Cygb*, and *Mpo*) and underexpressed one gene (*Fancc*) associated with antioxidant function (Table 2).

When the effects of NaI on oxidative stress-related gene transcription rates were examined in thyrocytes from each strain, the results were striking. In CBA/J thyrocytes, NaI upregulated the expression of 22 genes involved in antioxidant defense mechanisms and ROS metabolism, whereas the same treatment increased expression of only two of these genes (*Gpx2*, glutathionine peroxidase 2, and *Nqo1*, NADPH dehydrogenase, quinone 1) in NOD.H2^{h4} thyrocytes (Fig. 3). This gene set comprised several peroxidases, with the main effect observed with *Tpo* (thyroid peroxidase; 5.77-fold change). In contrast, NaI mildly upregulated the expression of only one gene (*Noxo1*, NADPH oxidase organizer 1; 2.09-fold change) and downregulated the expression of two genes *Cygb* (cytoglobin; −2.17-fold) and *Krt1* (keratin 1; −3.7-fold) in NOD.H2^{h4} cells. These results strongly suggest that an impaired capacity to mobilize molecules with antioxidant function might explain in part the observed susceptibility of NOD.H2^{h4} thyrocytes to apoptosis induced by low concentrations of NaI.

Discussion

The goal of this study was to examine whether NOD.H2^{h4} thyrocytes exhibit high sensitivity to NaI-induced apoptosis with the view that this might provide an early trigger in ISAT development in this mouse strain. Work with thyrocytes from euthyroid mice and relatively low doses of NaI could model *in vivo* processes of protracted increased dietary iodine intake in healthy people, and in this regard this approach differs from numerous previous studies that have described iodide-induced cell death in thyrocytes from goitrous animals (26). Our data show that NOD.H2^{h4} thyrocytes, cultured for 24 h in the presence of $4–8\times10^{-6}$ M NaI, underwent apoptosis at very high rates (40–55%), whereas similar treatment of thyrocytes from CBA/J mice—which are resistant to ISAT (23)—did not raise apoptosis above background levels. To our knowledge, such high levels of apoptosis induced by very low concentrations of iodide *in vitro* have not been previously reported. Previous studies with porcine (27) or human (21) thyroid follicles have shown pro-apoptotic effects of iodide in the $2–5\times10^{-6}$ M range, but the observed apoptotic rates were low (4–5%). Usually, very high levels ($10^{-4}–10^{-2}$ M) of iodide have been used to induce significant cell death in thyroid cell lines such as FRTL-5 cells (22,28), TAD-2 cells (20), or

Table 2. Differential Expression Levels of Oxidative Stress-Related Genes in NOD.H2^{h4} and CBA/J Thyrocytes

RefSeq	*Symbol*	*Description*	*Fold change (NOD.H2^{h4}/CBA/J)*[a]
Genes encoding proteins involved in ROS metabolism			
NM_010876	Ncf1	Neutrophil cytosolic factor 1	4.52
NM_010877	Ncf2	Neutrophil cytosolic factor 2	2.89
NM_013653	Ccl5	Chemokine (C-C motif) ligand 5	2.40
NM_001099297	Duox1	Dual oxidase 1	−2.74
Genes encoding proteins with antioxidant function			
NM_030677	Gpx2	Glutathione peroxidase 2	2.88
NM_030206	Cygb	Cytoglobin	2.51
NM_010824	Mpo	Myeloperoxidase	2.00
NM_007985	Fancc	Fanconi anemia, complementation group C	−4.78

[a]A fold change ≥2.00 (upregulation) and ≤ −2.00 (downregulation) was considered significant.

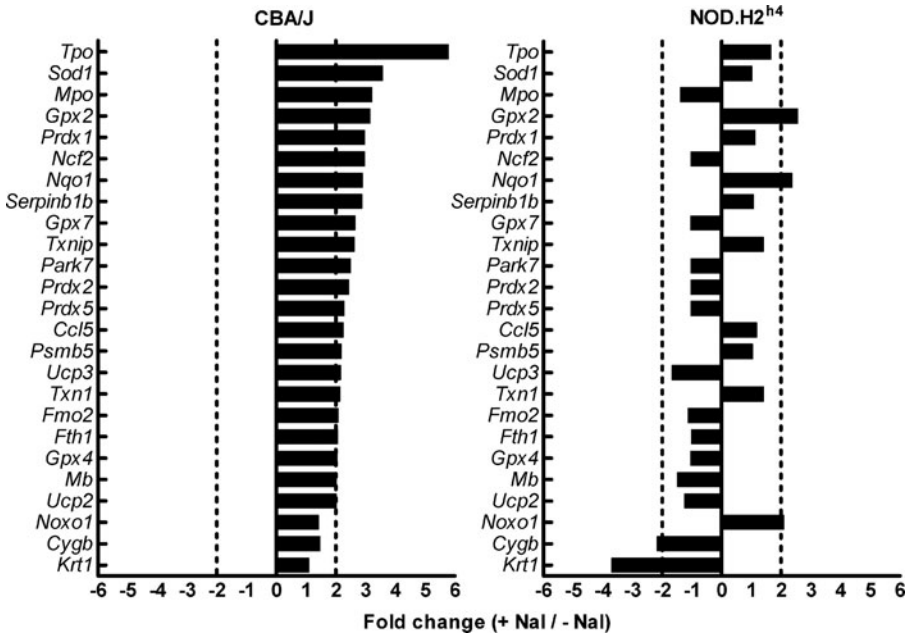

FIG. 3. Differential expression of oxidative stress-related genes in iodide-treated NOD.H2^{h4} and CBA/J thyrocytes. Thyroid cell suspensions from 80 NOD.H2^{h4} and 80 CBA/J thyroid glands were cultured *in vitro* for 9 days. On day 9, 4×10^{-6} M NaI was added to wells, and RNA was isolated 24 h later. cDNA was used in an Oxidative Stress PCR array and analyzed by real time PCR. Fold change ≥ 2.00 or ≤ -2.00 was considered significant.

human thyroid follicles (19). To a certain extent, variances in apoptotic rates reported by various studies may be due to the use of different assays of apoptosis measurement or even the animal species examined (28). Also, some functions, for example iodide inhibition of TSH-stimulated cAMP levels (29) as well as TPO bioactivity (30), could be altered when thyrocytes are cultured as mono-layers.

In this study, the enhanced NaI-induced cell death of NOD.H2^{h4} thyrocytes cannot be attributed to necrosis, since the levels of necrotic cells in all groups did not exceed 3.4%. The irreversible binding of the fluorescent inhibitor FAM-VAD-FMK to activated caspases 1, 3, 4, 5, 6, 7, 8, and 9 precludes speculation about the possible apoptotic pathways involved, for example the participation of the inflammasome via activation of caspase -1 or the apoptosome followed by activation of caspase 9 (31). Given the extent of apoptosis observed microscopically, it was surprising that the NaI treatment was found not to up- or downregulate any genes in the apoptotic gene array involved in the intrinsic and extrinsic apoptotic pathways, as well as in caspase and DNA damage response cascades, strongly suggesting that this process is independent of regulation at the transcription level and that it is executed by proteins already present in the cell. This finding is in agreement with data from a previous study showing that increasing concentrations of cycloheximide, a protein synthesis inhibitor, did not block the apoptosis of the iodide-treated thyroid cell line TAD-2 (20). Expression of *p53*, *Bcl-2*, *Bax*, and *Bcl-XL* genes has also been reported to remain unchanged at the protein level after 12, 24, and 48 h of KI treatment of TAD-2 cells (20), while gene array analysis in NIS/TPO modified lung cancer cells has shown that iodide-induced apoptosis did not alter significantly the expression levels of all apoptosis-related genes except *p21* and *survivin* (32). In our study, the apoptotic gene array data derived from NOD.H2^{h4} and CBA/J thyrocytes at the basal (non NaI-treated) state (Table 1) did not provide clear evidence that NOD.H2^{h4} thyrocytes exhibit an intrinsic defect favoring induction of apoptosis, since simultaneous mild over- or underexpression of apoptosis-promoting or inhibiting genes was detected in the thyrocytes from both strains. It remains open whether the iodolipid δ-lactone, which has been isolated from porcine thyroid follicles (33) as well as human thyroid tissue from patients with Graves' disease treated with high doses of iodide (34), has an active role in the apoptosis mechanism operating in our system. Both iodine and δ-lactone have been reported to induce apoptosis in porcine (27) as well as human thyroid follicles (21) and in the thyroid carcinoma cell line B-CPAP (35) through the mitochondrial pathway.

Thyroid epithelial cells are constantly exposed to ROS because they produce large amounts of H_2O_2 required for iodination of thyroglobulin. Since high levels of ROS can lead to oxidative damage, thyrocytes have protective mechanisms to control the intracellular levels of ROS (36,37). Defects in these regulatory networks have been proposed to underlie the spontaneous thyroiditis onset in OS chickens (38). NOD.H2^{h4} thyrocytes, either in the basal state or after exposure to 10^{-4} M NaI *in vitro*, have previously been reported to overexpress ROS as compared to control BALB/c and B10.A thyrocytes (25). Our data suggest that the high sensitivity of NOD.H2^{h4} thyrocytes to apoptosis, induced by low levels of NaI *in vitro*, may be, in part, due to an impairment in the upregulation of antioxidant activity. Twenty-two out of 84 oxidative stress-related genes in the array showed mild (2.01–3.57-fold) but significant overexpression in CBA/J thyrocytes, which were resistant to apoptosis. Highest overexpression (5.77-fold) was observed with the *Tpo* (thyroid peroxidase) gene. This contrasts with findings from previous studies reporting either no effect of iodide treatment on *Tpo* expression (23,39,40) or even down-regulation of its expression (41,42) in thyroid cells or lines. The reasons for this discrepancy are unclear but may be due to the different protocols used.

Among the set of overexpressed genes encoding proteins with antioxidant function were several glutathione peroxidases (*Gpx2*, *Gpx4*, and *Gpx7*) and peroxiredoxins (*Prdx1*,

Prdx2, and *Prdx5*) as well as *Sod1* (superoxide dismutase 1) and *Txn1* (thioredoxin 1) (36). Interestingly, increased expression of *Gpx2*, *Txn1*, but not *Gpx4* has been previously reported in the rat PCCL3 thyroid cells after iodide treatment *in vitro* (40,43). Other identified genes were as follows. The *Ucp2*, *Ucp3*, encoding the uncoupling proteins 2 and 3, located in the inner mitochondrial membrane. *Ucp2* mainly functions to attenuate mitochondrial production of ROS (44), whereas *Ucp3* seems to protect mitochondria against lipid-induced oxidative stress (45). *Nqo1* (NAD(P)H dehydrogenase), quinone 1, encoding a detoxification enzyme that catalyzes reduction in quinines (46). *Park7* (Parkinson's disease associated protein) encoding a protein that stabilizes Nrf2, the master regulator of antioxidant genes (47) and protects mitochondria from oxidative stress (48). *Fth1* encoding the iron-storing protein ferritin that minimizes oxidative stress (49). *Serpinb1b* encoding an inhibitor of neutrophil serine proteases, with a strong anti-inflammatory activity (50). The ROS responsive genes *Ccl5*, encoding the chemokine (C-C motif) ligand 5, and *Psmb5*, encoding the proteasome subunit, beta type 5. *Mb*, encoding a protein involved in oxygen transportation with a described antioxidant function in cardiac muscle (51). *Fmo2*, encoding a NADPH-dependent enzyme involved in the oxidation of various xenobiotics (52). *Txnip*, encoding a protein inhibiting the function of Txn1 and promoting induction of ROS generation (53). Of particular interest was the upregulation of the gene *Ncf2* (*p67^{phox}*; neutrophil cytosolic factor) expression in CBA/J thyrocytes, encoding a subunit of the ROS-generating NADPH oxidase, since it has been similarly reported to increase in iodide-treated BALB/c thyrocytes but not in iodide-treated NOD.H2^{h4} thyrocytes (25). In the iodide-treated NOD.H2^{h4} group, the expression of two genes with antioxidant function, *Gpx2* and *Nqo1*, as well as *Noxo1*, encoding for a cytosolic subunit of NADPH oxidase, was upregulated. Significant downregulation was observed in the expression of *Krt1*, a ROS responsive gene and *Cygb*, encoding an oxygen transporter with an antioxidant function in neuronal cells (54). Since the apoptotic fate of a thyrocyte is defined by the balance between ROS production and catabolism, these data imply that activation of several genes encoding proteins with antioxidant function plays a main role in the differential apoptosis observed in our study.

The high sensitivity of NOD.H2^{h4} thyrocytes to apoptosis induced by low concentrations of NaI *in vitro* may have important implications for the mechanisms operating in ISAT development. Apoptotic cascades in thyrocytes could be triggered by iodide and not result simply by mononuclear cell infiltration of the gland, as described in other studies (18). The physiological iodine plasma levels in mice (55,56) as well as in humans (19) are estimated to be in the 10^{-7} M range, and it has been reported that when the iodine intake is very high—for example 20 mg/day in some Japanese populations— the plasma iodine can increase 100-fold (19,57,58). It is thus conceivable that the pro-apoptotic *in vitro* effects of NaI on NOD.H2^{h4} thyrocytes shown in the present study might reflect similar processes in ISAT when mice are given 0.05% NaI in water (3×10^{-3} M) for several weeks. The increased apoptotic death of NOD.H2^{h4} thyrocytes in combination with the defective clearance of apoptotic cells by macrophages that has been described in NOD mice (59,60)—and possibly present in NOD.H2^{h4} mice—could lead to an antigenic overload in thyroid draining lymph nodes and activation of thyroid antigen specific T cells as shown in the NOD system (61,62).

Acknowledgments

We thank Drs. J. Vanderluit, R. Russell, and M. Licursi, as well as A. Atoom, Y. Komatsu, and M. Hasan, for their help with the immunofluorescence microscopy and real time PCR work. This work was supported by a grant from the Canadian Institutes of Health Research to G.C. P.K. was supported in part by a stipend from Memorial University of Newfoundland.

Author Disclosure Statement

The authors have no conflicts of interest.

References

1. Podolin PL, Pressey A, DeLarato NH, Fischer PA, Peterson LB, Wicker LS 1993 I-E+nonobese diabetic mice develop insulitis and diabetes. J Exp Med **178:**793–803.
2. Burek CL, Rose NR 2008 Autoimmune thyroiditis and ROS. Autoimmun Rev **7:**530–537.
3. Wicker LS, Todd JA, Peterson LB 1995 Genetic control of autoimmune diabetes in the NOD mouse. Annu Rev Immunol **13:**179–200.
4. Kong YM, David CS, Lomo LC, Fuller BE, Motte RW, Giraldo AA 1997 Role of mouse and human class II transgenes in susceptibility to and protection against mouse autoimmune thyroiditis. Immunogenetics **46:**312–317.
5. Wicker LS 1997 Major histocompatibility complex-linked control of autoimmunity. J Exp Med **186:**973–975.
6. Hutchings PR, Verma S, Phillips JM, Harach SZ, Howlett S, Cooke A 1999 Both CD4(+) T cells and CD8(+) T cells are required for iodine accelerated thyroiditis in NOD mice. Cell Immunol **192:**113–121.
7. Vecchiatti SM, Guzzo ML, Caldini EG, Bisi H, Longatto-Filho A, Lin CJ 2013 Iodine increases and predicts incidence of thyroiditis in NOD mice: histopathological and ultrastructural study. Exp Ther Med **5:**603–607.
8. Allen EM, Appel MC, Braverman LE 1986 The effect of iodide ingestion on the development of spontaneous lymphocytic thyroiditis in the diabetes-prone BB/W rat. Endocrinology **118:**1977–1981.
9. Bagchi N, Brown TR, Urdanivia E, Sundick RS 1985 Induction of autoimmune thyroiditis in chickens by dietary iodine. Science **230:**325–327.
10. Bournaud C, Orgiazzi JJ 2003 Iodine excess and thyroid autoimmunity. J Endocrinol Invest **26:**49–56.
11. Konno N, Makita H, Yuri K, Iizuka N, Kawasaki K 1994 Association between dietary iodine intake and prevalence of subclinical hypothyroidism in the coastal regions of Japan. J Clin Endocrinol Metab **78:**393–397.
12. Markou K, Georgopoulos N, Kyriazopoulou V, Vagenakis AG 2001 Iodine-induced hypothyroidism. Thyroid **11:**501–510.
13. Braley-Mullen H, Sharp GC, Medling B, Tang H 1999 Spontaneous autoimmune thyroiditis in NOD.H-2h4 mice. J Autoimmun **12:**157–165.
14. Rasooly L, Burek CL, Rose NR 1996 Iodine-induced autoimmune thyroiditis in NOD-H-2h4 mice. Clin Immunol Immunopathol **81:**287–292.
15. Provenzano MJ, Domann F, Hefley L 2009 Cellular iodine transport: body distribution of the human sodium iodide symporter. In: Preedy, VR, Burrow, GN, Watson, RR (eds)

Comprehensive Handbook of Iodine. Nutritional, Biochemical, Pathological and Therapeutic Aspects. First edition. Academic Press, Waltham, MA, p 207.
16. Chen W, Man N, Shan Z, Teng W 2011 Effects of long-term exposure to iodine excess on the apoptosis of thyrocytes in Wistar rats. Exper Clin Endocrinol Diabetes **119:**1–8.
17. Li M, Boyages SC 1994 Iodide induced lymphocytic thyroiditis in the BB/W rat: evidence of direct toxic effects of iodide on thyroid subcellular structure. Autoimmunity **18:**31–40.
18. Teng X, Shan Z, Teng W, Fan C, Wang H, Guo R 2009 Experimental study on the effects of chronic iodine excess on thyroid function, structure, and autoimmunity in autoimmune-prone NOD.H-2h4 mice. Clin Exp Med **9:**51–59.
19. Many MC, Mestdagh C, van den Hove MF, Denef JF 1992 *In vitro* study of acute toxic effects of high iodide doses in human thyroid follicles. Endocrinology **131:**621–630.
20. Vitale M, Di Matola T, D'Ascoli F, Salzano S, Bogazzi F, Fenzi G, Martino E, Rossi G 2000 Iodide excess induces apoptosis in thyroid cells through a p53-independent mechanism involving oxidative stress. Endocrinology **141:** 598–605.
21. Lehmann P, Rank P, Hallfeldt KL, Krebs B, Gartner R 2006 Dose-related influence of sodium selenite on apoptosis in human thyroid follicles *in vitro* induced by iodine, EGF, TGF-beta, and H2O2. Biol Trace Elem Res **112:**119–130.
22. Yao X, Li M, He J, Zhang G, Wang M, Ma J, Sun Y, Zhang W, Li L 2012 Effect of early acute high concentrations of iodide exposure on mitochondrial superoxide production in FRTL cells. Free Radic Biol Med **52:**1343–1352.
23. Li HS, Carayanniotis G 2007 Induction of goitrous hypothyroidism by dietary iodide in SJL mice. Endocrinology **148:**2747–2752.
24. Jeker LT, Hejazi M, Burek CL, Rose NR, Caturegli P 1999 Mouse thyroid primary culture. Biochem Biophys Res Commun **257:**511–515.
25. Sharma R, Traore K, Trush MA, Rose NR, Burek CL 2008 Intracellular adhesion molecule-1 up-regulation on thyrocytes by iodine of non-obese diabetic.H2(h4) mice is reactive oxygen species-dependent. Clin Exp Immunol **152:** 13–20.
26. Ruwhof C, Drexhage HA 2001 Iodine and thyroid autoimmune disease in animal models. Thyroid **11:**427–436.
27. Langer R, Burzler C, Bechtner G, Gartner R 2003 Influence of iodide and iodolactones on thyroid apoptosis. Evidence that apoptosis induced by iodide is mediated by iodolactones in intact porcine thyroid follicles. Exp Clin Endocrinol Diabetes **111:**325–329.
28. Golstein J, Dumont JE 1996 Cytotoxic effects of iodide on thyroid cells: difference between rat thyroid FRTL-5 cell and primary dog thyrocyte responsiveness. J Endocrinol Invest **19:**119–126.
29. Rapoport B, Adams RJ, Rose M 1977 Cultured thyroid cell adenosine 3′,5′-cyclic monophosphate response to thyrotropin: loss and restoration of sensitivity to iodide inhibition. Endocrinology **100:**755–764.
30. Magnusson RP, Rapoport B 1985 Modulation of differentiated function in cultured thyroid cells: thyrotropin control of thyroid peroxidase activity. Endocrinology **116:**1493–1500.
31. Latz E, Xiao TS, Stutz A 2013 Activation and regulation of the inflammasomes. Nat Rev Immunol **13:**397–411.
32. Zhang L, Sharma S, Zhu LX, Kogai T, Hershman JM, Brent GA, Dubinett SM, Huang M 2003 Nonradioactive iodide effectively induces apoptosis in genetically modified lung cancer cells. Cancer Res **63:**5065–5072.
33. Dugrillon A, Bechtner G, Uedelhoven WM, Weber PC, Gartner R 1990 Evidence that an iodolactone mediates the inhibitory effect of iodide on thyroid cell proliferation but not on adenosine 3′,5′-monophosphate formation. Endocrinology **127:**337–343.
34. Dugrillon A, Uedelhoven WM, Pisarev MA, Bechtner G, Gartner R 1994 Identification of delta-iodolactone in iodide treated human goiter and its inhibitory effect on proliferation of human thyroid follicles. Horm Metab Res **26:**465–469.
35. Gartner R, Rank P, Ander B 2010 The role of iodine and delta-iodolactone in growth and apoptosis of malignant thyroid epithelial cells and breast cancer cells. Hormones (Athens) **9:**60–66.
36. Schweizer U, Chiu J, Kohrle J 2008 Peroxides and peroxide-degrading enzymes in the thyroid. Antioxid Redox Signal **10:**1577–1592.
37. Smyth PP 2003 Role of iodine in antioxidant defence in thyroid and breast disease. Biofactors **19:**121–130.
38. Bagchi N, Brown TR, Herdegen DM, Dhar A, Sundick RS 1990 Antioxidants delay the onset of thyroiditis in obese strain chickens. Endocrinology **127:**1590–1595.
39. Kawashima A, Yamazaki K, Hara T, Akama T, Yoshihara A, Sue M, Tanigawa K, Wu H, Ishido Y, Takeshita F, Ishii N, Sato K, Suzuki K 2013 Demonstration of innate immune responses in the thyroid gland: potential to sense danger and a possible trigger for autoimmune reactions. Thyroid **23:**477–487.
40. Leoni SG, Galante PA, Ricarte-Filho JC, Kimura ET 2008 Differential gene expression analysis of iodide-treated rat thyroid follicular cell line PCCl3. Genomics **91:**356–366.
41. Morand S, Chaaraoui M, Kaniewski J, Deme D, Ohayon R, Noel-Hudson MS, Virion A, Dupuy C 2003 Effect of iodide on nicotinamide adenine dinucleotide phosphate oxidase activity and Duox2 protein expression in isolated porcine thyroid follicles. Endocrinology **144:**1241–1248.
42. Muller K, Krohn K, Eszlinger M, Ludgate M, Fuhrer D 2011 Effect of iodine on early stage thyroid autonomy. Genomics **97:**94–100.
43. Leoni SG, Kimura ET, Santisteban P, De la Vieja A 2011 Regulation of thyroid oxidative state by thioredoxin reductase has a crucial role in thyroid responses to iodide excess. Mol Endocrinol **25:**1924–1935.
44. Pi J, Zhang Q, Fu J, Woods CG, Hou Y, Corkey BE, Collins S, Andersen ME 2010 ROS signaling, oxidative stress and Nrf2 in pancreatic beta-cell function. Toxicol Appl Pharmacol **244:**77–83.
45. Liu J, Li J, Li WJ, Wang CM 2013 The role of uncoupling proteins in diabetes mellitus. J Diabetes Res 2013:585897.
46. Nioi P, McMahon M, Itoh K, Yamamoto M, Hayes JD 2003 Identification of a novel Nrf2-regulated antioxidant response element (ARE) in the mouse NAD(P)H:quinone oxidoreductase 1 gene: reassessment of the ARE consensus sequence. Biochem J **374:**337–348.
47. Clements CM, McNally RS, Conti BJ, Mak TW, Ting JP 2006 DJ-1, a cancer- and Parkinson's disease-associated protein, stabilizes the antioxidant transcriptional master regulator Nrf2. Proc Natl Acad Sci U S A **103:**15091–15096.
48. Ma Q 2013 Role of nrf2 in oxidative stress and toxicity. Annu Rev Pharmacol Toxicol **53:**401–426.
49. Hintze KJ, Theil EC 2005 DNA and mRNA elements with complementary responses to hemin, antioxidant inducers,

and iron control ferritin-L expression. Proc Natl Acad Sci U S A **102:**15048–15052.
50. Polytarchou C, Pfau R, Hatziapostolou M, Tsichlis PN 2008 The JmjC domain histone demethylase Ndy1 regulates redox homeostasis and protects cells from oxidative stress. Mol Cell Biol **28:**7451–7464.
51. Flogel U, Godecke A, Klotz LO, Schrader J 2004 Role of myoglobin in the antioxidant defense of the heart. FASEB J **18:**1156–1158.
52. Gornicka A, Morris-Stiff G, Thapaliya S, Papouchado BG, Berk M, Feldstein AE 2011 Transcriptional profile of genes involved in oxidative stress and antioxidant defense in a dietary murine model of steatohepatitis. Antioxid.Redox Signal **15:**437–445.
53. Spindel ON, World C, Berk BC 2012 Thioredoxin interacting protein: redox dependent and independent regulatory mechanisms. Antioxid Redox Signal **16:**587–596.
54. Li D, Chen XQ, Li WJ, Yang YH, Wang JZ, Yu AC 2007 Cytoglobin up-regulated by hydrogen peroxide plays a protective role in oxidative stress. Neurochem Res **32:**1375–1380.
55. Bernstein SE 2007 Physiological characteristics. In: Green EL (ed) Biology of the Laboratory Mouse. Second edition. Dover Publications, Inc., New York, NY.
56. Taurog A, Chaikoff IL 1946 On the determination of plasma iodine. J Biol Chem **163:**313.
57. Nagataki S 1974 Effect of excess quantities of iodide. In: Greep RO, Astwwood EB (eds) Handbook of Physiology. American Physiological Society, Washington DC, pp 329–344.
58. Suzuki H 1980 Etiology of endemic goiter and iodide excess. In: Stanbury JB, Hetzel BS (eds) Endemic Goiter and Endemic Cretinism. Iodine Nutrition in Health and Disease. J. Wiley and Sons, New York, NY, pp 237–253.
59. Maree AF, Komba M, Finegood DT, Edelstein-Keshet L 2008 A quantitative comparison of rates of phagocytosis and digestion of apoptotic cells by macrophages from normal (BALB/c) and diabetes-prone (NOD) mice. J Appl Physiol **104:**157–169.
60. O'Brien BA, Geng X, Orteu CH, Huang Y, Ghoreishi M, Zhang Y, Bush JA, Li G, Finegood DT, Dutz JP 2006 A deficiency in the *in vivo* clearance of apoptotic cells is a feature of the NOD mouse. J Autoimmun **26:**104–115.
61. Turley S, Poirot L, Hattori M, Benoist C, Mathis D 2003 Physiological beta cell death triggers priming of self-reactive T cells by dendritic cells in a type-1 diabetes model. J Exp Med **198:**1527–1537.
62. Hoglund P, Mintern J, Waltzinger C, Heath W, Benoist C, Mathis D 1999 Initiation of autoimmune diabetes by developmentally regulated presentation of islet cell antigens in the pancreatic lymph nodes. J Exper Med **189:**331.

Address correspondence to:
George Carayanniotis, PhD
Faculty of Medicine
Memorial University of Newfoundland
St. John's
NL A1B 3V6
Canada

E-mail: gcarayan@mun.ca